Accelerated Publications

Evidence from Biosynthetically Incorporated Strontium and FTIR Difference Spectroscopy that the C-Terminus of the D1 Polypeptide of Photosystem II Does Not Ligate Calcium†

Melodie A. Strickler,‡ Lee M. Walker,‡ Warwick Hillier,§ and Richard J. Debus*,‡

Department of Biochemistry, University of California, Riverside, California 92521-0129, and Research School of Biological Sciences, Australian National University, GPO Box 475, Canberra, ACT, Australia 2601

Received April 8, 2005; Revised Manuscript Received May 15, 2005

ABSTRACT: Recent FTIR studies have provided evidence that the C-terminal α-COO^- group of the D1 polypeptide at D1-Ala344 is a unidentate ligand of a Mn ion in photosystem II [Chu, H.-A., Hiller, W., and Debus, R. J. (2004) *Biochemistry 43*, 3152−3166; Kimura, Y., Mizusawa, N., Yamanari, T., Ishii, A., and Ono, T.-A. (2005) *J. Biol. Chem. 280*, 2078−2083]. However, the FTIR data could not exclude Ca ligation. Furthermore, the recent ∼3.5 Å X-ray crystallographic structural model positions the α-COO^- group of D1-Ala344 near a Ca ion [Ferreira, K. N., Iverson, T. M., Maghlaoui, K., Barber, J., and Iwata, S. (2004) *Science 303*, 1831−1838]. Therefore, to conclusively establish whether the α-COO^- group of D1-Ala344 ligates Mn or Ca, the symmetric carboxylate stretching mode of the α-COO^- group of D1-Ala344 was identified in the S_2-*minus*-S_1 FTIR difference spectrum of PSII particles having Sr substituted for Ca. Cells of the cyanobacterium *Synechocystis* sp. PCC 6803 were propagated in media having Sr substituted for Ca and containing either L-[1-^{13}C]alanine or unlabeled (^{12}C) alanine. The S_2-*minus*-S_1 FTIR difference spectra of the purified PSII particles show that substituting Sr for Ca alters several carboxylate stretching modes, including some that may correspond to one or more metal ligands, but importantly does not alter the symmetric carboxylate stretching mode of the α-COO^- group of D1-Ala344. In unlabeled PSII particles, this mode appears at ∼1356 cm^{-1} in the S_1 state and at either ∼1337 or ∼1320 cm^{-1} in the S_2 state, irrespective of whether the PSII particles contain Ca or Sr. These data are inconsistent with Ca ligation and show, therefore, that the C-terminal α-COO^- group of the D1 polypeptide ligates a Mn ion. These data also show that substituting Ca with the larger Sr ion perturbs other unidentified carboxylate groups, at least one of which may ligate the Mn_4 cluster.

The catalytic site of water oxidation in photosystem II (PSII)[1] contains a cluster of four Mn ions and one Ca ion. The Mn_4 cluster accumulates oxidizing equivalents in response to light-induced electron transfer reactions within PSII, thereby serving as the interface between one-electron photochemistry and the four-electron process of water oxidation (for reviews, see refs *1*−*3*). The functional role of the Ca ion remains uncertain, but it may bind and activate a substrate water molecule for nucleophilic attack during O−O bond formation. During each catalytic cycle, the Mn_4 cluster cycles through five oxidation states termed S_n, where *n* denotes the number of oxidizing equivalents that have been stored ($n = 0-4$). The S_1 state predominates in dark-adapted samples. Most interpretations of XANES data have concluded that the S_1 state consists of two Mn(III) and two Mn(IV) ions and that the S_2 state consists of one Mn(III) and three Mn(IV) ions (for a review, see ref *4*). The S_4 state is a transient intermediate that reverts to the S_0 state with the concomitant release of O_2.

The amino acid residues that ligate the Mn_4 cluster are provided mainly by the D1 polypeptide, one of the core subunits of PSII. This ligation environment was predicted by mutagenesis studies (for a review, see ref *5*) and has been largely confirmed by recent X-ray crystallographic studies (*6*, *7*). However, uncertainty prevails over whether the Mn_4 cluster is ligated by the C-terminal carboxylate of the mature D1 polypeptide (the α-COO^- group of D1-Ala344). In the recent ∼3.2 Å ($R_{free} = 0.42$) X-ray crystallographic structural model (*7*), the α-COO^- group of D1-Ala344 is not assigned. In the recent ∼3.5 Å ($R_{free} = 0.346$) X-ray crystallographic

† Support for this work was provided by the National Science Foundation (Grant MCB 0111065 to R.J.D.). Additional support to W.H. was provided by the Human Frontiers Science Program (Grant RGP0029/2002).

* To whom correspondence should be addressed. Phone: (951) 827-3483. Fax: (951) 827-4434. E-mail: richard.debus@ucr.edu.

‡ University of California.

§ Australian National University.

[1] Abbreviations: Chl, chlorophyll; Cyt, cytochrome; EPR, electron paramagnetic resonance; EXAFS, extended X-ray absorption fine structure; FTIR, Fourier transform infrared; MES, 2-(*N*-morpholino)-ethanesulfonic acid; NTA, nitrilotriacetic acid; PSII, photosystem II; RH, relative humidity; XANES, X-ray absorption near edge structure.

10.1021/bi050653y CCC: $30.25
Published on Web 05/27/2005

structural model (*6*), the α-COO^- group of D1-Ala344 ligates no metal ion but is located near a Ca ion. On the basis of recent isotope-edited FTIR studies, the α-COO^- group of D1-Ala344 has been proposed to ligate a Mn ion whose charge increases during the $S_1 \rightarrow S_2$ transition (*8*, *9*). In the FTIR studies, the symmetric carboxylate stretching [$\nu_{sym}(COO^-)$] mode of D1-Ala344 in the S_1 and S_2 states was identified by propagating cells of the cyanobacterium *Synechocystis* sp. PCC 6803 in the presence of either L-[1-^{13}C]alanine or unlabeled (^{12}C) alanine and recording the S_2-*minus*-S_1 FTIR difference spectrum of the purified PSII particles (*8*, *9*). In the unlabeled PSII particles, the $\nu_{sym}(COO^-)$ mode of D1-Ala344 appeared at ~1356 cm^{-1} in the S_1 state and at ~1339 or ~1320 cm^{-1} in the S_2 state. These positions are downshifted by >40 cm^{-1} in the S_1 state and >60 cm^{-1} in the S_2 state from the position of the $\nu_{sym}(COO^-)$ mode of free ionic carboxylate groups in solution (1400−1412 cm^{-1}). These substantial downshifts are not caused by protonation or by strong hydrogen bonding of the carboxylate because the positions of the modes are incompatible with protonation (*10*, *11*) and because prolonged (>20 h) $^2H_2O-^1H_2O$ exchange does not substantially alter the $\nu_{sym}(COO^-)$ region of the spectrum (*12*, *13*). The only other plausible explanation of the substantial downshifts is that the α-COO^- group of D1-Ala344 is a unidentate ligand of a metal ion (*8*, *9*).

Does the α-COO^- group of D1-Ala344 ligate Mn or Ca? If it ligates Ca, then removing Ca should prevent the substantial ligation-induced downshifts of the $\nu_{sym}(COO^-)$ mode. The removal of Ca from PSII has been reported to produce no major change in the $\nu_{sym}(COO^-)$ region of the S_2-*minus*-S_1 FTIR difference spectrum (*14*−*16*). Therefore, it was concluded that the α-COO^- group of D1-Ala344 is a unidentate ligand of Mn rather than Ca (*8*). However, the control experiments that were presented in refs *14*−*16* did not include measurements of the residual Ca content of the Ca-depleted PSII samples, measurements that are notoriously difficult to perform. Because the C-terminus of the D1 polypeptide is positioned near a Ca ion in the recent ~3.5 Å X-ray crystallographic structural model (*6*), it has been proposed that the α-COO^- group of D1-Ala344 ligates Ca during some (*6*, *9*) or all (*17*) of the steps in the catalytic cycle.

In this study, we reinvestigated whether the α-COO^- group of D1-Ala344 ligates Mn or Ca. Because of the difficulties associated with reversibly extracting Ca from PSII in cyanobacteria (*18*), we chose to substitute Sr for Ca, and to perform this substitution biosynthetically. Of all the cations that can competitively replace Ca in PSII, only Sr is capable of supporting O_2 evolution (*19*−*22*), a feature that has been attributed to the similar electronegativities of Ca and Sr, and hence to their similar pK_a values of their water ligands (*22*). The biosynthetic substitution of Sr for Ca was recently demonstrated in PSII from *Thermosynechococcus elongatus* (*23*). Substituting Sr for Ca alters the EPR properties of the S_2 state, increasing the fraction of PSII that exhibits a $g \approx 4.1$ (*21*, *24*) or $g \approx 5.25$ (*25*) EPR signal and altering the appearance of the $g = 2$ multiline EPR signal (*20*, *21*, *23*−*25*). Substituting Sr for Ca also shifts a low-frequency S_2 state vibrational mode that has been assigned to a Mn−O−Mn structural unit from ~606 to ~618 cm^{-1} (*26*). These spectral changes show that substituting Sr for Ca subtly perturbs the structure of the Mn_4 cluster. Therefore, substituting Sr for Ca would be expected to alter the vibrational modes of multiple carboxylate residues that are located near, or ligated to, the Mn_4 cluster. Indeed, subtle changes in the $\nu_{sym}(COO^-)$ region of the S_2-*minus*-S_1 FTIR difference spectrum were reported previously in spinach PSII membranes that had been depleted of Ca and reconstituted with Sr (*15*).

To determine if the $\nu_{sym}(COO^-)$ mode of D1-Ala344 is altered by the substitution of Sr for Ca, cells of *Synechocystis* sp. PCC 6803 were propagated in media having Sr substituted for Ca and containing either L-[1-^{13}C]alanine or unlabeled (^{12}C) alanine. The S_2-*minus*-S_1 FTIR difference spectra of the resulting PSII particles show that substituting Sr for Ca alters several carboxylate stretching modes, including some that may correspond to one or more metal ligands, but does not alter the $\nu_{sym}(COO^-)$ mode of D1-Ala344. On the basis of these data, we conclude that the C-terminus of the D1 polypeptide does not ligate Ca.

MATERIALS AND METHODS

Propagation of Cultures. Wild-type cells of *Synechocystis* sp. PCC 6803 containing a hexahistidine tag on the C-terminus of CP47 were propagated as described previously (*8*, *27*). For the isolation of Sr-containing PSII, the $CaCl_2$ in the liquid medium was replaced with an equivalent concentration of $SrCl_2$ (*23*). For the isolation of isotopically labeled PSII, cells were propagated photoautotrophically in liquid medium containing 0.5 mM L-[1-^{13}C]alanine (99% ^{13}C enrichment, Cambridge Isotope Laboratories, Andover, MA), as described previously (*8*).

Purification of PSII Particles. Isolated PSII particles were purified under dim green light at 4 °C with Ni−NTA superflow affinity resin (Qiagen, Valentia, CA) as described previously (*27*) except that all buffers contained 1.2 M betaine and 10% (v/v) glycerol instead of 25% (v/v) glycerol (*23*). For the purification of Sr-containing PSII particles, all buffers contained $SrCl_2$ instead of $CaCl_2$.[2] Purified PSII particles were concentrated to 0.5−1.0 mg of Chl/mL by ultrafiltration, frozen in liquid nitrogen, and stored at −196 °C (vapor phase nitrogen).

EPR Measurements. Continuous-wave EPR spectra were recorded with a Bruker EMX Series X-band EPR spectrometer that was equipped with an ER-4119HS cavity. Cryogenic temperatures were obtained with an Oxford ESR900 liquid helium cryostat. The temperature was controlled with an Oxford ITC503 temperature and gas flow controller that was equipped with a Cernox (Lake Shore Cryotronics, Westerville, OH) temperature sensor. Sample manipulations were conducted under dim green light at 4 °C. The samples [in 1.2 M betaine, 10% (v/v) glycerol, 50 mM MES-NaOH (pH 6.0), 20 mM $CaCl_2$ or 20 mM $SrCl_2$, 5 mM $MgCl_2$, 50 mM histidine, 1 mM EDTA, and 0.03% (w/v) *n*-dodecyl *β*-D-maltoside] were concentrated to 6−10 mg of Chl/mL with Centricon-100 concentrators (Millipore Corp., Bedford, MA),

[2] Purification in buffers containing Ca yielded a mixed population of Sr-containing (≤75%) and Ca-containing (≥25%) PSII particles, as estimated from analyses of S_2 state multiline EPR signals (not shown). This partial exchange probably reflects weaker binding of Cyt c_{550} in *Synechocystis* sp. PCC 6803 than in *T. elongatus*. In the latter organism, biosynthetically incorporated Sr cannot be exchanged with Ca ions in solution (*23*).

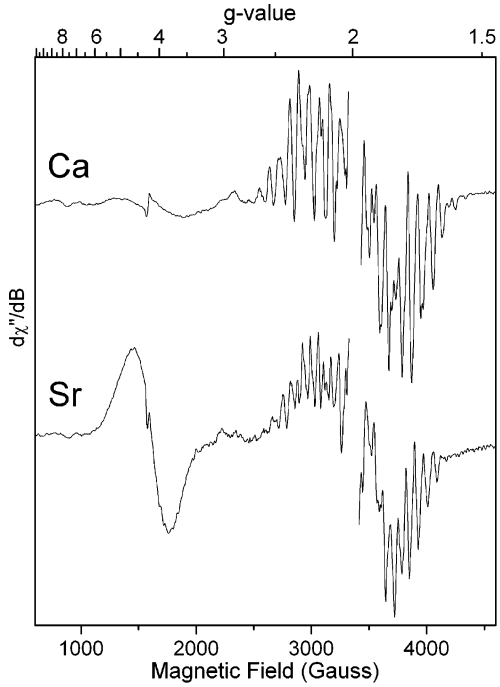

FIGURE 1: Light-*minus*-dark EPR spectra of PSII particles purified from *Synechocystis* sp. PCC 6803 cells that had been propagated in media containing Ca (top trace) or Sr (bottom trace). Both spectra have had the large $g = 2$ signal of $Y_D^{\bullet}$ excised for clarity. Samples were illuminated for 5 min at 198 K before being flash-frozen in liquid nitrogen. The Ca and Sr samples contained ~8 and ~7.4 mg of Chl/mL, respectively. The spacings of the hyperfine lines in the $g = 2$ multiline signals of the Ca-containing and Sr-containing PSII particles were 85 ± 9 and 68 ± 9 G, respectively. Experimental conditions: microwave frequency of 9.41 GHz, microwave power of 2 mW, modulation amplitude of 12 G, modulation frequency of 100 kHz, time constant of 41 ms, conversion time of 41 ms, and temperature of 7.5 ± 0.5 K. The Ca and Sr spectra represent the accumulations of 50 and 60 scans, respectively.

deaerated by being gently bubbled with a stream of Ar gas, transferred to standard quartz 4 mm OD EPR tubes (Wilmad LabGlass, Buena, NJ) under an atmosphere of Ar gas, dark-adapted for 30−60 min on ice, and then frozen in liquid nitrogen. The S_2 state was generated by illuminating samples for 5 min in a non-silvered Dewar at 198 K (dry ice/ethanol) with a focused, 250 W quartz tungsten halogen lamp (Oriel Corporation, Stratford, CT) whose output was filtered through 54 mm of H_2O and two heat-absorbing filters. The samples were then immediately frozen in liquid nitrogen. For each sample, the spectrum of the dark-adapted (S_1 state) sample was obtained after dark-adapting the illuminated sample on ice for 2 h.

FTIR Measurements. All manipulations were conducted under dim green light at 4 °C. For each FTIR sample, approximately 35 μg of Chl was concentrated to <15 μL with a Microcon-100 concentrator (Millipore Corp.). The concentrated sample was then diluted with 150 μL of FTIR buffer [40 mM sucrose, 10 mM MES-NaOH (pH 6.0), 5 mM $CaCl_2$ or 5 mM $SrCl_2$, 5 mM NaCl, and 0.06% (w/v) *n*-dodecyl β-D-maltoside (*27*, *28*)] and concentrated again. The sample was diluted and concentrated seven or eight additional times to remove all traces of betaine, with the final concentrated volume being approximately 10 μL (betaine has a number of strong IR absorption modes that interfere with the calculation of FTIR difference spectra). The concentrated sample was then mixed with $^1/_{10}$ volume of fresh 100 mM potassium ferricyanide (dissolved in water) and spread to a diameter of ~10 mm on a 15 mm diameter BaF_2 window. The sample was dried lightly (until tacky) under a stream of dry nitrogen gas and then placed in a humidifier at 95% RH for 10 min. A second IR window with a Teflon spacer (0.5 mm thick) was placed over the first and sealed with silicon-free high-vacuum grease. The sample was then loaded into the FTIR cryostat and allowed to equilibrate to 250.0 K in darkness for 2−4 h. The sample concentration was adjusted so that the absorbance of the amide I band at 1657 cm^{-1} was 0.6−0.9.

FTIR Spectra. Midfrequency FTIR spectra were recorded with a Bruker Equinox 55 spectrometer (Bruker Optics, Billerica, MA) as described previously (*8*). The spectral resolution for all spectra was 4 cm^{-1}. Samples were illuminated with a single flash (~20 mJ/flash, ~7 ns fwhm) from a frequency-doubled Q-switched Nd:YAG laser [Surelite I (Continuum, Santa Clara, CA)]. The single-beam

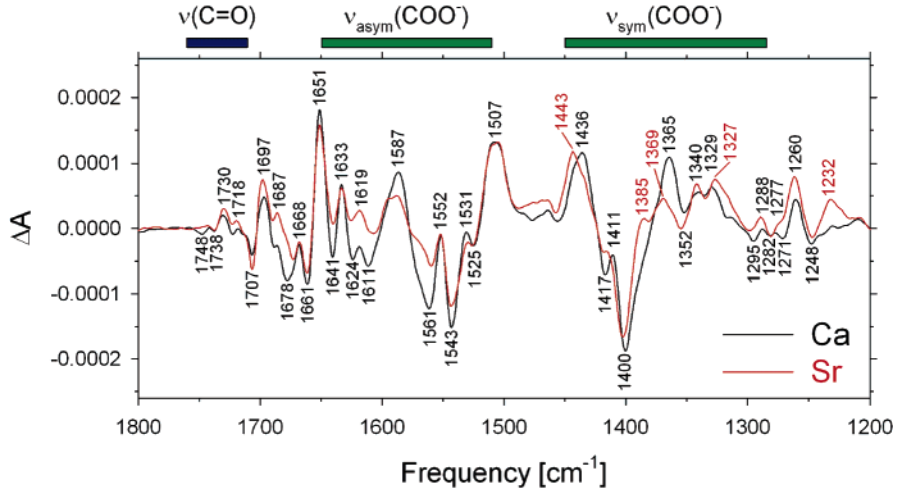

FIGURE 2: Comparison of the midfrequency (1800−1200 cm^{-1}) flash-induced S_2-*minus*-S_1 FTIR difference spectra of PSII particles purified from *Synechocystis* sp. PCC 6803 cells that had been propagated in media containing Ca (black) or Sr (red). Green bars denote the $\nu_{sym}(COO^-)$ and $\nu_{sym}(COO^-)$ regions of the spectra; a blue bar denotes the $\nu(C{=}O)$ region. Each trace represents the average of six samples. To facilitate comparison, the amplitude of the Sr spectrum was multiplied by a factor of ~1.4 after the spectra had been normalized to the peak-to-peak amplitudes of the negative ferricyanide peak at 2115 cm^{-1} and the positive ferrocyanide peak at 2038 cm^{-1}. The sample temperature was 250 K.

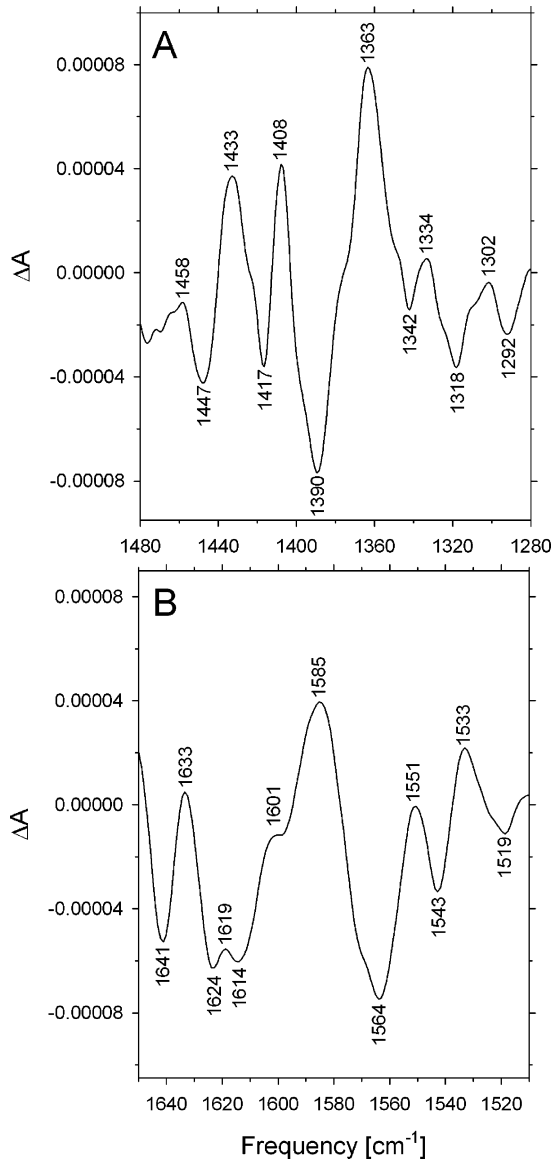

FIGURE 3: Double-difference spectrum, Ca-*minus*-Sr, of PSII particles obtained by subtracting the S_2-*minus*-S_1 FTIR difference spectrum of Sr-containing PSII particles from the S_2-*minus*-S_1 FTIR difference spectrum of Ca-containing PSII particles (the spectra shown in Figure 2 were subtracted directly without further adjustment). Panel A shows the symmetric carboxylate stretching [$\nu_{sym}(COO^-)$] region, while panel B shows the asymmetric carboxylate stretching [$\nu_{asym}(COO^-)$] region. The $\nu_{asym}(COO^-)$ region also contains amide I (1700−1610 cm^{-1}) and amide II (1565−1550 cm^{-1}) modes.

spectrum that was recorded after the flash was divided by the single-beam spectrum that was recorded before the flash, and the ratio was converted to units of absorption. Each single-beam spectrum consisted of 800 scans. Each sample was flash-illuminated only once. The spectra of multiple samples were averaged.

Other Procedures. Chlorophyll concentrations and light-saturated rates of O_2 evolution were measured as described previously (*8*).

RESULTS AND DISCUSSION

The O_2 evolving activities of the purified Ca- and Sr-containing wild-type PSII particles were 5.2−5.5 and 2.1−3.3 mmol of O_2 (mg of Chl)$^{-1}$ h^{-1}, respectively. The lower activity of Sr-containing PSII particles (40−60% compared to that of the Ca-containing PSII particles in this study) has been observed previously (e.g., refs *19*, *20*, *23*, and *29*) and can be attributed to a slowing of the individual S state transitions (*23*, *29*, *30*). The O_2 evolving activities were similar irrespective of whether the assay buffer contained Ca or Sr.

To confirm that Sr had replaced Ca in the Mn_4Ca cluster, the light-*minus*-dark EPR spectrum corresponding to the S_2 state was examined (Figure 1). The spectra show that substituting Sr for Ca induced a large $g \approx 4.1$ EPR signal and altered the appearance of the multiline $g = 2$ EPR signal by increasing the number of hyperfine lines, altering their intensity pattern, and decreasing their spacing from 85 ± 9 G in the Ca-containing PSII particles to 68 ± 9 G in the Sr-containing PSII particles. Previous studies have shown that substituting Sr for Ca increases the fraction of PSII that exhibits a $g \approx 4.1$ (*21*, *24*) or $g \approx 5.25$ (*25*) EPR signal and alters the appearance of the $g = 2$ multiline EPR signal in the manner that is observed in Figure 1, decreasing the spacing of the hyperfine lines from 84−90 to 66−71 G (e.g., refs *20*, *21*, and *23*−*25*). Therefore, propagating *Synechocystis* sp. PCC 6803 in media containing Sr instead of Ca results in substituting Sr for Ca in the Mn_4Ca cluster, in agreement with the recent study that was conducted with *T. elongatus* (*23*).

The midfrequency S_2-*minus*-S_1 FTIR difference spectra of Ca- and Sr-containing PSII particles are compared in Figure 2 (black and red spectra, respectively). The comparison shows that substituting Sr for Ca alters numerous vibrational modes in the $\nu_{sym}(COO^-)$ and $\nu_{asym}(COO^-)$ regions of the spectrum (1450−1280 and 1650−1510 cm^{-1}, respectively) and eliminates a weak negative band at ∼1748 cm^{-1}. The latter may arise from the carbonyl stretching [ν(C═O)] mode of a protonated carboxylate group (*10*, *11*), the ν(C═O) mode of the 10a ester carbonyl of a Chl *a* molecule (*31*), or a combination mode formed between two fundamental modes whose frequencies lie outside the ν(C═O) region. These alterations[3] are largely consistent with a previous study of biochemically substituted samples (*15*). However, the S_2-*minus*-S_1 FTIR difference spectra that were presented in the earlier study (*15*) were obtained by subtracting $Q_A^{\bullet-}$-*minus*-Q_A difference spectra from $S_2Q_A^{\bullet-}$-*minus*-S_1Q_A difference spectra, leading to potential uncertainty in the S_2-*minus*-S_1 difference spectra, especially in the $\nu_{sym}(COO^-)$ region. Furthermore, no Ca-*minus*-Sr difference spectrum was reported (*15*). In our data (Figure 2), the Sr-containing samples appear to contain a slightly larger population of Mn-depleted PSII than the Ca-containing samples. This is evident from the larger amplitudes of the (−)1707 and (+)1697 cm^{-1} bands and the more pronounced shoulder at (+)1600 cm^{-1} in the Sr-containing samples. These modes are characteristic of the $Y_D^{\bullet}$-*minus*-Y_D FTIR

[3] These alterations are not caused by the presence of potassium ions (*15*) because replacing potassium ferricyanide with tetrabutylammonium ferricyanide had no effect on the spectra (not shown). Because the Sr-containing PSII particles were isolated and analyzed in the presence of exogenous Sr ions, we cannot exclude the possibility that some of the alterations are caused by Sr ions that are bound weakly outside the catalytic site. However, this possibility seems unlikely because the FTIR difference spectra reflect only those structural perturbations that are caused by the accumulation of an oxidizing equivalent on the Mn_4 cluster.

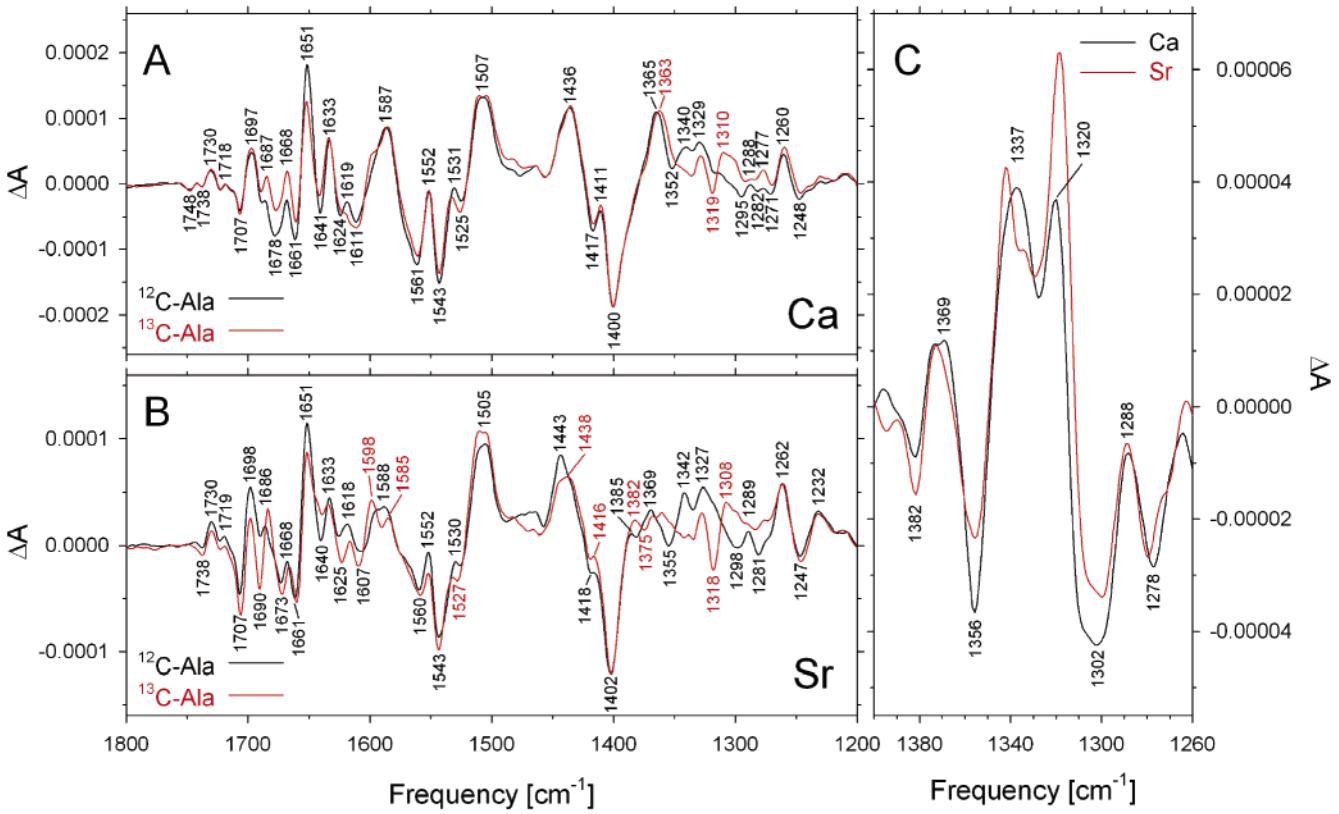

FIGURE 4: Comparison of the midfrequency (1800−1200 cm^{-1}) flash-induced S_2-*minus*-S_1 FTIR difference spectra of PSII particles purified from *Synechocystis* cells that had been propagated in media containing Ca (A) or Sr (B) and either unlabeled (^{12}C) L-alanine (black traces) or L-[1-^{13}C]alanine (red traces). The spectra of the unlabeled PSII particles are the same as those shown in Figure 2 but have been normalized to the peak-to-peak amplitudes of the negative ferricyanide peak at 2115 cm^{-1} and the positive ferrocyanide peak at 2038 cm^{-1}. Each trace represents the average of six samples. Within each panel, the spectra have been normalized to maximize their overlap between 1500 and 1400 cm^{-1}. The sample temperature was 250 K. Panel C shows the double-difference spectra, ^{12}C-*minus*-^{13}C, of PSII particles containing Ca (black trace) or Sr (red trace) obtained by subtracting the S_2-*minus*-S_1 FTIR difference spectra of L-[1-^{13}C]alanine-labeled PSII particles from the S_2-*minus*-S_1 FTIR difference spectra of unlabeled PSII particles (the spectra shown in panels A and B were subtracted directly without further adjustment). Only the regions between 1400 and 1260 cm^{-1} are shown.

difference spectrum that is exhibited by Mn-depleted PSII centers when illuminated under the current experimental conditions (*8*). A larger proportion of Mn-depleted PSII in the Sr-containing samples might be expected because of weaker binding of Cyt c_{550} in Sr-containing PSII (*23*) and the increased lability of the Mn_4 cluster in *Synechocystis* sp. PCC 6803 in the absence of this polypeptide (*32*). The $Y_D^{\bullet}$-*minus*-Y_D FTIR difference spectrum of *Synechocystis* sp. PCC 6803 shows only weak absorption features in the $\nu_{sym}(COO^-)$ region (*8*, *33*, *34*). Therefore, the significant Sr-induced alterations in the $\nu_{sym}(COO^-)$ modes (Figure 2) are not caused by a greater proportion of Mn-depleted PSII centers in the Sr-containing samples.

To display more clearly the $\nu_{sym}(COO^-)$ and $\nu_{asym}(COO^-)$ modes that are shifted by the substitution of Sr for Ca, the Ca-*minus*-Sr double-difference spectra for the $\nu_{sym}(COO^-)$ and $\nu_{asym}(COO^-)$ regions are shown in panels A and B of Figure 3, respectively. These double-difference spectra confirm that substituting Sr for Ca alters numerous $\nu_{sym}(COO^-)$ modes and probably alters several $\nu_{asym}(COO^-)$ modes, although distinguishing some of the latter from altered amide I or amide II modes would require additional isotopic labeling experiments (amide I and amide II modes appear at 1700−1610 and 1565−1550 cm^{-1}, respectively). The large number of altered carboxylate modes shows that the oxidation of Mn that occurs during the $S_1 \rightarrow S_2$ transition is structurally coupled to the Ca cofactor and provides further support for an intimate connection between Ca and the Mn_4 cluster. The features that appear in Figure 3A at frequencies of >1400 cm^{-1} may correspond to free carboxylate groups; the features that appear at frequencies of <1400 cm^{-1} may correspond to one or more unidentate carboxylate metal ligands (*8*). The Sr-induced spectral shifts are probably caused by the larger ionic radius of Sr [132 pm for six-coordinate Sr^{2+} vs 114 pm for six-coordinate Ca^{2+} (*35*)] and the higher pK_a of its water ligands [12.70 for Ca vs 13.18 for Sr (*22*, *35*)]. The larger size of Sr would likely perturb the structure of the Mn_4 cluster, whereas the decreased acidity of Sr-bound water would weaken the hydrogen bonds that are formed by these ligands (*36*), thereby perturbing the hydrogen bond networks that are maintained by Ca. Perturbations of the structure of the Mn_4 cluster would shift the $\nu_{sym}(COO^-)$ modes of unidentate carboxylate metal ligands, while perturbations of hydrogen bond networks would alter the $\nu_{sym}(COO^-)$ and $\nu_{asym}(COO^-)$ modes of free carboxylates. A Sr-induced shift of a mode that appears in the S_2-*minus*-S_1 FTIR difference spectrum should yield two resolved or partially resolved differential peaks in the Ca-*minus*-Sr double difference spectrum. However, the complexity of the double-difference spectra shown in panels A and B of Figure 3 precludes assigning relationships between individual peaks. Nevertheless, from the numerous positive and negative features that are present in these spectra, it is evident that the substitution of Sr for Ca alters the $\nu_{sym}(COO^-)$ modes of at least two

carboxylate residues, at least one of which probably ligates a metal ion.[4]

To determine if the vibrational modes in the S_2-*minus*-S_1 FTIR difference spectrum that are shifted by Sr include the $\nu_{sym}(COO^-)$ mode of the α-COO^- group of D1-Ala344, the position of this mode was visualized by purifying PSII particles from cells that had been propagated in media containing L-[1-^{13}C]alanine. A comparison of the midfrequency S_2-*minus*-S_1 FTIR difference spectra of Ca- and Sr-containing PSII particles containing either unlabeled (^{12}C) alanine (black traces) or L-[1-^{13}C]alanine (red traces) is shown in panels A and B of Figure 4. One notable difference in the L-[1-^{13}C]alanine-induced alterations in the Ca- and Sr-containing samples is the larger amplitude of the positive peak at ~1598 cm^{-1} in the labeled Sr-containing sample (Figure 4B). This peak has been attributed to the fraction of PSII centers that lost the Mn_4 cluster during purification (*8*). Aside from the probable differences in the fractions of inactive (Mn-depleted) PSII, the data show that the incorporation of L-[1-^{13}C]alanine induced similar changes in Ca- and Sr-containing PSII particles in the $\nu_{sym}(COO^-)$ region except for some small changes in the Sr-containing samples (e.g., near ~1438 and ~1382 cm^{-1} in the labeled sample) that are not understood at this time and will be the subject of future investigation.

To display the L-[1-^{13}C]alanine-shifted $\nu_{sym}(COO^-)$ modes more clearly, the ^{12}C-*minus*-^{13}C double-difference spectra of the region between 1400 and 1260 cm^{-1} in the Ca- and Sr-containing samples are presented in Figure 4C. The data show that the positions of the L-[1-^{13}C]alanine-shifted modes in the S_1 and S_2 states are nearly identical in the Ca- and Sr-containing samples. In both samples, the data are consistent with a single S_1 state mode at ~1356 cm^{-1} in the unlabeled samples shifting to ~1337 or ~1320 cm^{-1} after the incorporation of L-[1-^{13}C]alanine and with a single S_2 state mode at ~1320 or ~1337 cm^{-1} shifting to ~1302 cm^{-1}. These L-[1-^{13}C]alanine-shifted modes were observed previously in Ca-containing wild-type PSII particles from *Synechocystis* sp. PCC 6803 and were shown to originate from the $\nu_{sym}(COO^-)$ mode of the α-COO^- group of D1-Ala344 (*8*, *9*).[5]

The data of Figure 4C show that substituting Sr for Ca does not shift the $\nu_{sym}(COO^-)$ mode of D1-Ala344 significantly in either the S_1 or S_2 state. However, substituting Sr for Ca *does* perturb the structure of the Mn_4 cluster as shown by the Sr-induced alterations in the EPR signals of the S_2 state (Figure 1 and refs *20*, *21*, and *23*−*25*), by the Sr-induced shift of the ~606 cm^{-1} vibrational mode that has been assigned to a Mn−O−Mn structural unit (*26*), and by the Sr-induced shift of several unassigned $\nu_{sym}(COO^-)$ and $\nu_{asym}(COO^-)$ modes (Figures 2 and 3). The conformational states of the Mn_4 cluster that give rise to the $g = 2$ multiline and $g \approx 4.1$ signals in the S_2 state are believed to differ in terms of the valence distribution of the Mn_4 cluster or the spin state of the Mn(III) ion that is present in the S_2 state (*37*, *38*). The S_2-*minus*-S_1 FTIR difference spectra of PSII preparations that exhibit difference proportions of the $g = 2$ multiline and $g \approx 4.1$ EPR signals are essentially identical (*39*). Therefore, the Sr-induced shifts of the $\nu_{sym}(COO^-)$ modes do not arise from a Sr-induced change in the fraction of PSII that exhibits the $g = 2$ multiline EPR signal and are unlikely to arise simply from a change in the valence distribution of the Mn_4 cluster. Rather, the Sr-induced shifts must reflect Sr-induced structural perturbations.

It seems highly improbable that the perturbations of the Mn_4 cluster that are induced by substituting Sr for Ca would not also alter the $\nu_{sym}(COO^-)$ mode of a carboxylate residue that directly coordinates the Ca ion. Because substituting Sr for Ca does not alter the $\nu_{sym}(COO^-)$ mode of D1-Ala344 (Figure 4C), we conclude that the C-terminal carboxylate group of the D1 polypeptide does not ligate Ca. Therefore, because this carboxylate group must be a unidentate ligand of a metal ion (*8*, *9*), it must ligate a Mn ion. This conclusion conflicts with the recent ~3.5 Å X-ray crystallographic structural model of PSII (*6*). In this model, the α-COO^- group of D1-Ala344 does not ligate Mn but instead is positioned close to a Ca ion. However, XANES and EXAFS analyses of PSII single crystals show that the high doses of X-rays that were employed for recording the diffraction data (*6*, *7*) would have caused significant damage to the Mn_4 cluster by reducing the Mn ions to their Mn(II) oxidation states (V. K. Yachandra, personal communication). Consequently, the positions of at least some of the Mn ions in the recent X-ray crystallographic structural models (*6*, *7*) may not correspond to their true positions in intact PSII.

[4] The shift of a single $\nu_{sym}(COO^-)$ mode that appears in the S_2-*minus*-S_1 FTIR difference spectrum could give rise to up to four peaks in the double-difference spectrum, two positive and two negative, as shown by the double-difference spectra that are presented in Figure 4C.

[5] Specific L-[1-^{13}C]alanine labeling of PSII shifts the $\nu_{sym}(COO^-)$ mode of the α-COO^- group of D1-Ala344 by either ~19 or ~36 cm^{-1} (*8*). It is not yet possible to distinguish between these two possibilities.

ACKNOWLEDGMENT

We are grateful to Alain Boussac for advice concerning the propagation of cyanobacteria in media having Sr substituted for Ca, to Anh P. Nguyen for maintaining the cultures of *Synechocystis* sp. PCC 6803 and for purifying the thylakoid membranes that were used for purifying the PSII particles, to David F. Bocian for helpful discussions, and to the reviewers for helpful comments about the manuscript.

REFERENCES

1. Goussias, C., Boussac, A., and Rutherford, A. W. (2002) Photosystem II and Photosynthetic Oxidation of Water: An Overview, *Philos. Trans. R. Soc. London, Ser. B 357*, 1369−1381.
2. Vrettos, J. S., and Brudvig, G. W. (2004) Oxygen Evolution, *Compr. Coord. Chem. II 8*, 507−547.
3. Hillier, W., and Messinger, J. (2005) Mechanism of Photosynthetic Oxygen Production, in *Photosystem II: The Water/Plastoquinone Oxido-Reductase in Photosynthesis* (Wydrzynski, T., and Satoh, Ki., Eds.) Springer, Dordrecht, The Netherlands (in press).
4. Yachandra, V. K. (2005) The Catalytic Manganese Cluster, in *Photosystem II: The Water/Plastoquinone Oxido-Reductase in Photosynthesis* (Wydrzynski, T., and Satoh, Ki., Eds.) Springer, Dordrecht, The Netherlands (in press).
5. Debus, R. J. (2005) The Catalytic Manganese Cluster. II. Protein Ligation, in *Photosystem II: The Water/Plastoquinone Oxido-Reductase in Photosynthesis* (Wydrzynski, T., and Satoh, Ki., Eds.) Springer, Dordrecht, The Netherlands (in press).
6. Ferreira, K. N., Iverson, T. M., Maghlaoui, K., Barber, J., and Iwata, S. (2004) Architecture of the Photosynthetic Oxygen-Evolving Center, *Science 303*, 1831−1838.
7. Biesiadka, J., Loll, B., Kern, J., Irrgang, K.-D., and Zouni, A. (2004) Crystal Structure of Cyanobacterial Photosystem II at 3.2

Å Resolution: A Closer Look at the Mn-Cluster, *Phys. Chem. Chem. Phys. 6*, 4733−4736.
8. Chu, H.-A., Hillier, W., and Debus, R. J. (2004) Evidence that the C-Terminus of the D1 Polypeptide is Ligated to the Manganese Ion that Undergoes Oxidation During the S_1 to S_2 Transition: An Isotope-Edited FTIR Study, *Biochemistry 43*, 3152−3166.
9. Kimura, Y., Mizusawa, N., Yamanari, T., Ishii, A., and Ono, T.-A. (2005) Structural Changes of D1 C-terminal α-Carboxylate during S-state Cycling of Photosynthetic Oxygen Evolution, *J. Biol. Chem. 280*, 2078−2083.
10. Venyaminov, S. Yu., and Kalnin, N. N. (1990) Quantitative IR Spectrophotometry of Peptide Compounds in Water (H_2O) Solutions. 1. Spectral Parameters of Amino Acid Residue Absorption Bands, *Biopolymers 30*, 1243−1257.
11. Barth, A. (2000) The Infrared Absorption of Amino Acid Side Chains, *Prog. Biophys. Mol. Biol. 74*, 141−173.
12. Noguchi, T., Ono, T.-A., and Inoue, Y. (1995) A Carboxylate Ligand Interacting with Water in the Oxygen-Evolving Center of Photosystem II as Revealed by Fourier Transform Infrared Spectroscopy, *Biochim. Biophys. Acta 1232*, 59−66.
13. Noguchi, T., and Sugiura, M. (2002) FTIR Detection of Water Reactions During the Flash-Induced S-State Cycle of the Photosynthetic Water-Oxidizing Complex, *Biochemistry 41*, 15706−15712.
14. Kimura, Y., and Ono, T.-A. (2001) Chelator-Induced Disappearance of Carboxylate Stretching Vibrational Modes in S_2/S_1 FTIR Spectrum in Oxygen-Evolving Complex of Photosystem II, *Biochemistry 40*, 14061−14068.
15. Kimura, Y., Hasegawa, K., and Ono, T.-A. (2002) Characteristic Changes of the S_2/S_1 Difference FTIR Spectrum Induced by Ca^{2+} Depletion and Metal Cation Substitution in the Photosynthetic Oxygen-Evolving Complex, *Biochemistry 41*, 5844−5853.
16. Kimura, Y., and Ono, T.-A. (2003) Functional and Structural Study on Chelator-Induced Suppression of S_2/S_1 FTIR Spectrum in Photosynthetic Oxygen-Evolving Complex, *J. Inorg. Biochem. 97*, 231−239.
17. McEvoy, J. P., and Brudvig, G. W. (2004) Structure-Based Mechanism of Photosynthetic Water Oxidation, *Phys. Chem. Chem. Phys. 6*, 4754−4763.
18. Pauly, S., Schlodder, E., and Witt, H. T. (1992) The Influence of Salts on Charge Separation ($P_{680}{}^{+}Q_A{}^{-}$) and Water Oxidation of Photosystem II Complexes from Thermophilic Cyanobacteria: Active and Inactive Conformational States of Photosystem II, *Biochim. Biophys. Acta 1099*, 203−210.
19. Ghanotakis, D. F., Babcock, G. T., and Yocum, C. F. (1984) Calcium Reconstitutes High Rates of Oxygen Evolution in Polypeptide Depleted Photosystem II Preparations, *FEBS Lett. 167*, 127−130.
20. Boussac, A., and Rutherford, A. W. (1988) S-State Formation after Ca^{2+} Depletion in the Photosystem II Oxygen-Evolving Complex, *Chem. Scripta 28A*, 123−126.
21. Ono, T.-A., and Inoue, Y. (1989) Roles of Ca^{2+} in O_2 Evolution in Higher Plant Photosystem II: Effects of Replacement of Ca^{2+} Site by Other Cations, *Arch. Biochem. Biophys. 275*, 440−448.
22. Vrettos, J. S., Stone, D. A., and Brudvig, G. W. (2001) Quantifying the Ion Selectivity of the Ca^{2+} Site in Photosystem II: Evidence for Direct Involvement of Ca^{2+} in O_2 formation, *Biochemistry 40*, 7937−7945.
23. Boussac, A., Rappaport, F., Carrier, P., Verbavatz, J.-M., Gobin, R., Kirilovsky, D., Rutherford, A. W., and Sugiura, M. (2004) Biosynthetic Ca^{2+}/Sr^{2+} Exchange in the Photosystem II Oxygen-Evolving Enzyme of *Thermosynechococcus elongatus*, *J. Biol. Chem. 279*, 22809−22819.
24. Boussac, A., and Rutherford, A. W. (1988) Nature of the Inhibition of the Oxygen-Evolving Enzyme of Photosystem II by NaCl Washing and Reversed by the Addition of Ca^{2+} or Sr^{2+}, *Biochemistry 27*, 3476−3483.
25. Boussac, A., Sugiura, M., Inoue, Y., and Rutherford, A. W. (2000) EPR Study of the Oxygen Evolving Complex in His-Tagged Photosystem II from the Cyanobacterium *Synechococcus elongatus*, *Biochemistry 39*, 13788−13799.
26. Chu, H.-A., Sackett, H., and Babcock, G. T. (2000) Identification of a Mn−O−Mn Cluster Vibrational Mode of the Oxygen-Evolving Complex in Photosystem II by Low-Frequency FTIR Spectroscopy, *Biochemistry 39*, 14371−14376.
27. Debus, R. J., Strickler, M. A., Walker, L. M., and Hillier, W. (2005) No Evidence from FTIR Difference Spectroscopy That Aspartate-170 of the D1 Polypeptide Ligates a Manganese Ion That Undergoes Oxidation during the S_0 to S_1, S_1 to S_2, or S_2 to S_3 Transitions in Photosystem II, *Biochemistry 44*, 1367−1374.
28. Yamanari, T., Kimura, Y., Mizusawa, N., Ishii, A., and Ono, T.-A. (2004) Mid- to Low-Frequency Fourier Transform Infrared Spectra of S-State Cycle for Photosynthetic Water Oxidation in *Synechocystis* sp. PCC 6803, *Biochemistry 43*, 7479−7490.
29. Westphal, K. L., Lydakis-Simantiris, N., Cukier, R. I., and Babcock, G. T. (2000) Effects of Sr^{2+}-Substitution on the Reduction Rates of $Y_Z^{\bullet}$ in PSII Membranes: Evidence for Concerted Hydrogen-Atom Transfer in Oxygen Evolution, *Biochemistry 39*, 16220−16229.
30. Boussac, A., Sétif, P., and Rutherford, A. W. (1992) Inhibition of Tyrosine Z Photooxidation after Formation of the S_3-State in Ca^{2+}-Depleted and Cl^{-}-Depleted Photosystem II, *Biochemistry 31*, 1224−1234.
31. Nabedryk, E., Leonhard, M., Mäntele, W., and Breton, J. (1990) Fourier Transform Infrared Difference Spectroscopy Shows No Evidence for an Enolization of Chlorophyll *a* upon Cation Formation either in Vitro or during P700 Photooxidation, *Biochemistry 29*, 3242−3247.
32. Shen, J. R., Qian, M., Inoue, Y., and Burnap, R. L. (1998) Functional Characterization of *Synechocystis* sp. PCC 6803 Δ*psb*U and Δ*psb*V Mutants Reveals Important Roles of Cytochrome *c*-550 in Cyanobacterial Oxygen Evolution, *Biochemistry 37*, 1551−1558.
33. Hienerwadel, R., Boussac, A., Breton, J., Diner, B. A., and Berthomieu, C. (1997) Fourier Transform Infrared Difference Spectroscopy of Photosystem II Tyrosine D Using Site-Directed Mutagenesis and Specific Isotope Labeling, *Biochemistry 36*, 14712−14723.
34. Noguchi, T., Inoue, Y., and Tang, X. S. (1997) Structural Coupling Between the Oxygen-Evolving Mn Cluster and a Tyrosine Residue in Photosystem II as Revealed by Fourier Transform Infrared Spectroscopy, *Biochemistry 36*, 14705−14711.
35. Huheey, J. E., Keiter, E. A., and Keiter, R. L. (1993) *Inorganic Chemistry: Principles of Structure and Reactivity*, 4th ed., HarperCollins College Publishers, New York.
36. Riggs-Gelasco, P. J., Mei, R., Ghanotakis, D. F., Yocum, C. F., and Penner-Hahn, J. E. (1996) X-ray Absorption Spectroscopy of Calcium-Substituted Derivatives of the Oxygen-Evolving Complex of Photosystem II, *J. Am. Chem. Soc. 118*, 2400−2410.
37. Boussac, A., Girerd, J.-J., and Rutherford, A. W. (1996) Conversion of the Spin State of the Manganese Complex in Photosystem II Induced by Near-Infrared Light, *Biochemistry 35*, 6984−6989.
38. Boussac, A. (1997) Inhomogeneity of the EPR Multiline Signal from the S_2-State of the Photosystem II Oxygen-Evolving Enzyme, *JBIC, J. Biol. Inorg. Chem. 2*, 580−585.
39. Onoda, K., Mino, H., Inoue, Y., and Noguchi, T. (2000) An FTIR study on the structure of the oxygen-evolving Mn-cluster of Photosystem II in different spin forms of the S_2 state, *Photosynth. Res. 63*, 47−57.

BI050653Y